Inorg. Chem. **2004**, *43*, 964–968

Inorganic Chemistry

Article

Synthesis, Structure, and Characterization of Two New Layered Mixed-Metal Phosphates, $BaTeMO_4(PO_4)$ (M = Nb^{5+} or Ta^{5+})

Kang Min Ok, Joseph Orzechowski, and P. Shiv Halasyamani*

*Department of Chemistry and Center for Materials Chemistry, 136 Fleming Building,
University of Houston, Houston, Texas 77204-5003*

Received September 3, 2003

Two new isostructural mixed-metal phosphates, $BaTeMO_4(PO_4)$ (M = Nb^{5+} or Ta^{5+}), have been synthesized as bulk phase powders and single crystals by standard solid-state techniques using $BaCO_3$, TeO_2, Nb_2O_5 (or Ta_2O_5), and $NH_4H_2PO_4$ as reagents. The materials have novel layered crystal structures consisting of $[M^{5+}O_{6/2}]^-$ corner-sharing octahedral chains that are connected to $[Te^{4+}O_{4/2}]^0$ polyhedra and $[P^{5+}O_{2/1}O_{2/2}]^-$ tetrahedra. The Ba^{2+} cations reside between the layers and maintain charge balance. The Te^{4+} cations are in asymmetric coordination environments attributable to their lone pairs. The Nb^{5+} distorts along the local C_4 direction of its octahedron resulting in a "short–long–short–long" Nb–O–Nb bond motif. The Nb^{5+} cation displaces away from the oxide ligands that are bonded to Te^{4+} or P^{5+} cations, attributable to the structural rigidity of the TeO_4 and PO_4 polyhedra. Thus, the TeO_4 and PO_4 polyhedra support and reinforce the intraoctahedral distortion observed within the NbO_6 octahedra. Infrared and Raman spectroscopy, thermogravimetric analysis, and ion-exchange experiments are also presented. Crystal data: $BaTeNbO_4(PO_4)$, orthorhombic, space group *Pbca* (No. 61), with $a = 6.7351(9)$ Å, $b = 7.5540(10)$ Å, $c = 27.455(4)$ Å, $V = 1396.8(3)$ Å^3, and $Z = 8$; $BaTeTaO_4(PO_4)$, orthorhombic, space group *Pbca* (No. 61), with $a = 6.734(2)$ Å, $b = 7.565(3)$ Å, $c = 27.435(9)$ Å, $V = 1372.6(8)$ Å^3, and $Z = 8$.

Introduction

Transition metal oxyphosphates have received considerable attention attributable to their fascinating structural chemistry.[1–4] The rich structural chemistry can be attributed to the different building blocks, i.e., metal oxide octahedra and phosphate tetrahedra, observed in the materials. The diverse coordination geometry results in the formation of a wide variety of structural topologies, e.g., one-dimensional chains,[5,6] two-dimensional layers,[7–9] and three-dimensional frameworks.[10–12] Moreover, the various compounds exhibit very interesting materials properties such as electric,[13–15] magnetic,[16,17] catalytic,[17] and second-harmonic generating properties.[18–20] The other interesting building blocks are cations with lone pairs (Pb^{2+}, Bi^{3+}, Sb^{3+}, Te^{4+}, and Se^{4+}). These cations are found in a variety of asymmetric and variable coordination environments attributable to their lone pair. The lone pair is thought to be the result of a second-order Jahn–Teller

---

* To whom correspondence should be addressed. E-mail: psh@uh.edu. Phone: 713-743-3278. Fax: 713-743-2787.

(1) Berrah, F.; Mezaoui, D.; Guesdon, A.; Borel, M. M.; Leclaire, A.; Provost, J. *Chem. Mater.* **1998**, *10*, 543.
(2) Guesdon, A.; Raveau, B. *Chem. Mater.* **2000**, *12*, 2239.
(3) Sassoye, C.; Norton, K.; Sevov, S. C. *Inorg. Chem.* **2003**, *42*, 1652.
(4) Mayer, H.; Weil, M. *Z. Anorg. Allg. Chem.* **2003**, *629*, 1068.
(5) Zid, M. F.; Jouini, T.; Jouini, N. *C. R. Acad. Sci., Ser. IIc: Chim.* **1989**, *309*, 343.
(6) Borel, M. M.; Leclaire, A.; Chardon, J.; Michel, C.; Provost, J.; Raveau, B. *J. Solid State Chem.* **1998**, *135*, 302.
(7) Fakhfakh, M.; Zid, M. F.; Jouini, N.; Tournoux, M. *J. Solid State Chem.* **1993**, *102*, 368.
(8) Hoareau, T.; Leclaire, A.; Borel, M. M.; Grandin, A.; Raveau, B. *J. Solid State Chem.* **1995**, *116*, 87.
(9) Borel, M. M.; Leclaire, A.; Chardon, J.; Provost, J.; Raveau, B. *J. Solid State Chem.* **1998**, *137*, 214.
(10) Fakhfakh, M.; Verbaere, A.; Jouini, N. *Eur. J. Solid State Inorg. Chem.* **1992**, *29*, 563.
(11) Fakhfakh, M.; Ammar-Merah, S.; Jouini, N. *Solid State Sci.* **2000**, *2*, 587.
(12) Leclaire, A.; Chardon, J.; Provost, J.; Raveau, B. *J. Solid State Chem.* **2002**, *163*, 308.
(13) Ledain, S.; Leclaire, A.; Borel, M. M.; Provost, J.; Raveau, B. *J. Solid State Chem.* **1998**, *140*, 128.
(14) Leclaire, A.; Chardon, J.; Boudin, S.; Provost, J.; Raveau, B. *Chem. Mater.* **2002**, *14*, 3427.
(15) Fakhfakh, M.; Madani, A.; Jouini, N. *Mater. Res. Bull.* **2003**, *38*, 1215.
(16) Das, B. B.; Benhamada, L.; Grandin, A.; Borel, M. M.; Leclaire, A.; Raveau, B. *Mater. Chem. Phys.* **1995**, *39*, 239.
(17) Boudin, S.; Guesdon, A.; Leclaire, A.; Borel, M.-M. *Int. J. Inorg. Mater.* **2000**, *2*, 561.
(18) Tordjman, I.; Masse, R.; Guitel, J. C. *Z. Kristallogr.* **1974**, *139*, 103.
(19) Liang, C. S.; Harrison, W. T. A.; Eddy, M. M.; Gier, T. E.; Stucky, G. D. *Chem. Mater.* **1993**, *5*, 917.
(20) Gopalakrishnan, J.; Ramesha, K.; Kasthuri Rangan, K.; Pandey, S. *J. Solid State Chem.* **1999**, *148*, 75.

10.1021/ic0350335 CCC: $27.50

distortion.[21−25] The addition of these variable coordination geometries, e.g., trigonal-pyramid, seesaw, or square-pyramid, to the octahedral or tetrahedral moieties in the framework may result in novel structural topologies. One aspect of the materials that we hope to gain a better understanding of concerns the intraoctahedral distortion of the d^0 transition metal cation. This distortion is a driving force, in noncentrosymmetric materials, for a variety of important materials properties including piezoelectricity, ferroelectricity, and second-harmonic generation. We are trying to understand the influence of other metal oxide polyhedra, e.g., tetrahedra and distorted polyhedra, on the intraoctahedral distortion. With these ideas in mind, we investigated materials in the Ba−M−P−oxide system (M = Nb or Ta). In this paper, we report the synthesis, structure, and characterization of two new layered materials, $BaTeMO_4(PO_4)$ (M = Nb or Ta).

Experimental Section

Reagents. $(NH_4)H_2PO_4$ (Aldrich, 98+%), $BaCO_3$ (Aldrich, 99+%), Nb_2O_5 (Aldrich, 99.99%), Ta_2O_5 (Alfa Aeser, 99%), and TeO_2 (Aldrich, 99%) were used as received.

Synthesis. $BaTeMO_4(PO_4)$ (M = Nb or Ta) were synthesized through standard solid-state techniques. A stoichiometric mixture of $BaCO_3$ (0.987 g, 5.00×10^{-3} mol), Nb_2O_5 (or Ta_2O_5) (0.665 g (or 1.105 g for Ta_2O_5), 2.50×10^{-3} mol), $(NH_4)H_2PO_4$ (0.575 g, 5.00×10^{-3} mol), and TeO_2 (0.798 g, 5.00×10^{-3} mol) was thoroughly ground and pressed into a pellet. The pellet was heated in air to 500, 550, 650, and 750 °C for 12 h at each temperature with intermediate regrindings. Powder X-ray diffraction patterns on the resultant white powder indicated the material was single-phase and in agreement with the generated pattern from the single-crystal data (see Supporting Information). Crystals of $BaTeNbO_4(PO_4)$ were prepared by placing a mixture of $BaCO_3$ (0.197 g, 1.00×10^{-3} mol), Nb_2O_5 (0.266 g, 1.00×10^{-3} mol), $(NH_4)H_2PO_4$ (0.115 g, 1.00×10^{-3} mol), and TeO_2 (1.277 g, 8.00×10^{-3} mol) into a platinum crucible. The mixture was gradually heated in air to 750 °C, held for 15 h, and then cooled slowly to 550 °C at 6 °C h^{-1} before being quenched to room temperature. Crystals of $BaTeNbO_4(PO_4)$ (colorless blocks; 74% yield based on Nb_2O_5) were recovered with TeO_2 from the crucible. Since a pure bulk phase powder of $BaTeTaO_4(PO_4)$ could be synthesized successfully, powder X-ray diffraction was used to show $BaTeTaO_4(PO_4)$ is isostructural to $BaTeNbO_4(PO_4)$.

Crystallographic Determination. The structure of $BaTeNbO_4(PO_4)$ was determined by standard crystallographic methods. A colorless block ($0.02 \times 0.03 \times 0.05$ mm^3) was used for single-crystal measurement. Room temperature intensity data were collected on a Siemens SMART diffractometer equipped with a 1 K CCD area detector using graphite monochromated Mo Kα radiation. A hemisphere of data was collected using a narrow-frame method with scan widths of 0.30° in ω, and an exposure time of 30 s/frame. The first 50 frames were remeasured at the end of the data collection to monitor instrument and crystal stabilities. The maximum correction applied to the intensities was <1%. The data were integrated using the Siemens SAINT program,[26] with the intensities corrected for Lorentz, polarization, air absorption, and absorption attributable to the variation in the path length through the detector faceplate. ψ-Scans were used for the absorption correction on the hemisphere of data. The data were solved and refined using SHELXS-97 and SHELXL-97, respectively.[27,28] All atoms were refined with anisotropic thermal parameters and converged for $I > 2\sigma(I)$. All calculations were performed using the WinGX-98 crystallographic software package.[29] Crystallographic data and selected bond distances for $BaTeNbO_4(PO_4)$ are given in Tables 1 and 2, with additional details found in the Supporting Information.

Table 1. Crystallographic Data for $BaTeNbO_4(PO_4)$

chemical formula	$BaTeNbO_4(PO_4)$
fw	516.82
space group	*Pbca* (No. 61)
a (Å)	6.7351(9)
b (Å)	7.5540(10)
c (Å)	27.455(4)
V (Å^3)	1396.8(3)
Z	8
T (°C)	293.0(2)
λ (Å)	0.71073
ρ_{calcd} (g cm^{-3})	4.915
μ (Mo Kα) (cm^{-1})	115.75
$R(F)^a$	0.0285
$R_w(F_o^2)^b$	0.0465

[a] $R(F) = \sum||F_o| - |F_c||/\sum|F_o|$. [b] $R_w(F_o^2) = [\sum w(F_o^2 - F_c^2)^2/\sum w(F_o^2)^2]^{1/2}$.

Table 2. Selected Bond Distances (Å) for $BaTeNbO_4(PO_4)$

Nb(1)−O(1)	2.038(4)	Te(1)−O(1)	1.899(4)	P(1)−O(4)	1.561(5)
Nb(1)−O(2)	1.800(4)	Te(1)−O(3)	1.890(4)	P(1)−O(6)	1.550(4)
Nb(1)−O(2)	2.110(4)	Te(1)−O(5)	1.932(4)	P(1)−O(7)	1.526(5)
Nb(1)−O(3)	1.970(4)	Te(1)−O(6)	2.313(4)	P(1)−O(8)	1.519(5)
Nb(1)−O(4)	2.069(4)				
Nb(1)−O(5)	1.886(4)				

Powder Diffraction. The X-ray powder diffraction data were collected on a Scintag XDS2000 diffractometer at room temperature (Cu Kα radiation, $\theta-\theta$ mode, flat plate geometry) equipped with Peltier germanium solid-state detector in the 2θ range 3−110° with a step size of 0.02°, and a step time of 10 s. For $BaTeTaO_4(PO_4)$, the unit cell was determined by using the program ERACEL.[30] The unit cell, d_{obs}, d_{calc}, I_{obs}, and I_{calc} for $BaTeTaO_4(PO_4)$ are given in Table 3.

Infrared and Raman Spectroscopy. Infrared spectra were recorded on a Matteson FTIR 5000 spectrometer in the 400−4000 cm^{-1} range, with the sample pressed between two KBr pellets. Raman spectra were recorded at room temperature on a Digilab FTS 7000 spectrometer equipped with a germanium detector with the powder sample placed in separate capillary tubes. Excitation was provided by a Nd:YAG laser at a wavelength of 1064 nm, and the output laser power was 500 mW. The spectral resolution was about 4 cm^{-1}, and 200 scans were collected for each sample.

Thermogravimetric Analysis. Thermogravimetric analyses were carried out on a TGA 2950 thermogravimetric analyzer (TA

---

(21) Opik, U.; Pryce, M. H. L. *Proc. R. Soc. London* **1957**, *A238*, 425.
(22) Bader, R. F. W. *Mol. Phys.* **1960**, *3*, 137.
(23) Bader, R. F. W. *Can. J. Chem.* **1962**, *40*, 1164.
(24) Pearson, R. G. *J. Mol. Struct.: THEOCHEM* **1983**, *103*, 25.
(25) Wheeler, R. A.; Whangbo, M.-H.; Hughbanks, T.; Hoffmann, R.; Burdett, J. K.; Albright, T. A. *J. Am. Chem. Soc.* **1986**, *108*, 2222.
(26) *SAINT; Version 4.05 ed.: Program for Area Detector Absorption Correction*; Siemens Analytical X-ray Instruments: Madison, WI, 1995.
(27) Sheldrick, G. M. *SHELXS-97—A program for automatic solution of crystal structures*; University of Goettingen: Goettingen, Germany, 1997.
(28) Sheldrick, G. M. *SHELXL-97—A program for crystal structure refinement*; University of Goettingen: Goettingen, Germany, 1997.
(29) Farrugia, L. J. *J. Appl. Crystallogr.* **1999**, *32*, 837.
(30) Laugier, J.; Filhol, A. *ERACEL—A program for refinement of the cell parameters*; 1978.

Table 3. Powder X-ray Diffraction Data for $BaTeTaO_4(PO_4)^a$

h	k	l	d_{obs}	d_{calc}	I_{obs}	I_{calc}	h	k	l	d_{obs}	d_{calc}	I_{obs}	I_{calc}
0	0	2	13.702	13.718	30	43	1	1	8	2.834	2.833	3	4
1	0	2	6.043	6.045	3	1	1	2	5	2.825	2.827	21	31
1	0	4	4.806	4.805	12	11	0	2	7	2.723	2.722	6	7
0	0	6	4.570	4.573	38	32	2	0	6	2.711	2.711	36	42
1	1	5	3.710	3.708	7	12	2	2	1	2.504	2.504	5	9
0	0	8	3.429	3.429	100	100	1	2	9	2.238	2.239	15	20
2	0	0	3.368	3.367	6	9	3	1	2	2.126	2.126	1	1
1	2	1	3.275	3.274	79	93	3	1	6	1.947	1.947	1	1
1	0	8	3.057	3.056	2	2	3	2	1	1.925	1.926	20	25

[a] Refined unit cell (calculated using the atomic coordinates for $BaNbTeO_4(PO_4)$ but substituting tantalum for niobium): $a = 6.734(2)$ Å, $b = 7.565(3)$ Å, $c = 27.435(9)$ Å, $\alpha = \beta = \gamma = 90°$; space group *Pbca* (No. 61).

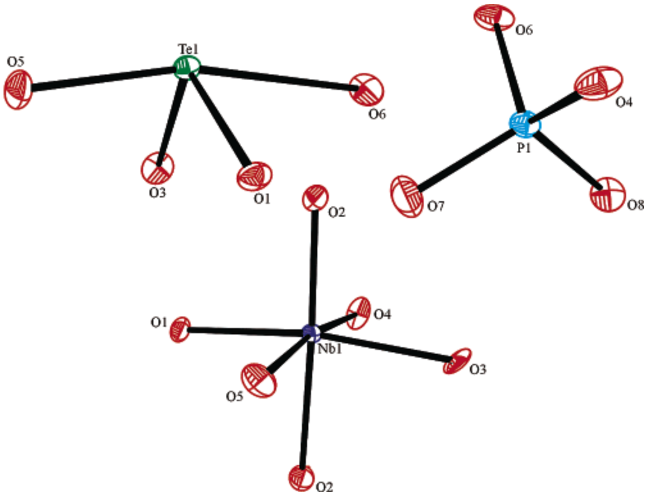

Figure 1. ORTEP (50% probability ellipsoids) for the asymmetric TeO_4 polyhedra, PO_4 tetrahedra, and NbO_6 octahedra in $BaTeNbO_4(PO_4)$.

Instruments). The samples were contained within platinum crucibles and heated at a rate of 10 °C min^{-1} from room temperature to 900 °C in nitrogen.

Ion-Exchange Experiments. Ion-exchange reactions were attempted by two different methods. The first method was carried out by stirring ca. 100 mg of polycrystalline $BaTeMO_4(PO_4)$ (M = Nb or Ta) in 5 mL of 1 M aqueous solution of the $Ca(NO_3)_2$ and $Sr(NO_3)_2$. The aqueous solution mixture was heated to 80 °C for 3 days. The second method was performed by heating ca. 100 mg of polycrystalline samples with ca. 500 mg of $CaCl_2$ (or $SrCl_2$) and 1 mL of H_2O in sealed fused silica tubes. The tubes were heated to 120 °C for 4 days. The products from each ion-exchange reaction method were recovered by filtration, washed with excess H_2O, and dried in air for 1 day.

Results and Discussion

Structures. Since the materials reported in this paper are isostructual, only the structural details of $BaTeNbO_4(PO_4)$ will be given. $BaTeNbO_4(PO_4)$ exhibits a two-dimensional layered structure consisting of asymmetric TeO_4 polyhedra, PO_4 tetrahedra, and NbO_6 octahedra (see Figure 1). The Te^{4+} cations are in a distorted “seesaw” environment, bonded to four oxygen atoms. The Te−O bond distances range from 1.890(4) to 2.313(4) Å with O−Te−O bond angles ranging from 81.31(16)° to 166.51(18)°. The asymmetric TeO_4 groups link two NbO_6 octahedra in an intrachain manner through O(1) and O(3). In addition, interchain connections are made by TeO_4 groups through O(5) and O(6) to NbO_6 and PO_4 groups, respectively. The PO_4 tetrahedra are connected to a niobium and a tellurium atom through O(4) and O(6), respectively. The PO_4 groups cap the NbO_6 and TeO_4 groups together from above and below to “complete” each layer. The P−O bond distances range from 1.519(5) to 1.561(5) Å. The Nb^{5+} cations are in octahedral coordination bonded to six oxygen atoms, with a cationic displacement from the center of the octahedron in the local C_4 direction that results in one “short” (1.800(4) Å), one “long” (2.110(4) Å), and four “normal” (∼2.00 Å) Nb−O bonds. Each NbO_6 octahedron shares corners through O(2), forming a chain along the *b*-axis. Thus a “short−long−short−long” Nb−O−Nb bond motif is observed. The four other corners of the NbO_6 octahedra, i.e., the “normal” Nb−O bonds, are connected to one phosphorus and three tellurium atoms. The Ba^{2+} cations are in 10-fold coordination environments with Ba−O contacts ranging from 2.748(4) to 3.248(4) Å. In connectivity terms, the structure can be described as an anionic layer, $\{[Nb^{5+}O_{6/2}]^{-}[Te^{4+}O_{4/2}]^{0}[P^{5+}O_{2/1}O_{2/2}]^{-}\}^{2-}$, with charge neutrality maintained by the Ba^{2+} cation (see Figure 2). Bond valence calculations[31,32] on $BaTeNbO_4(PO_4)$ resulted in values of 1.89, 4.03, 5.22, and 4.94 for Ba^{2+}, Te^{4+}, Nb^{5+}, and P^{5+}, respectively.

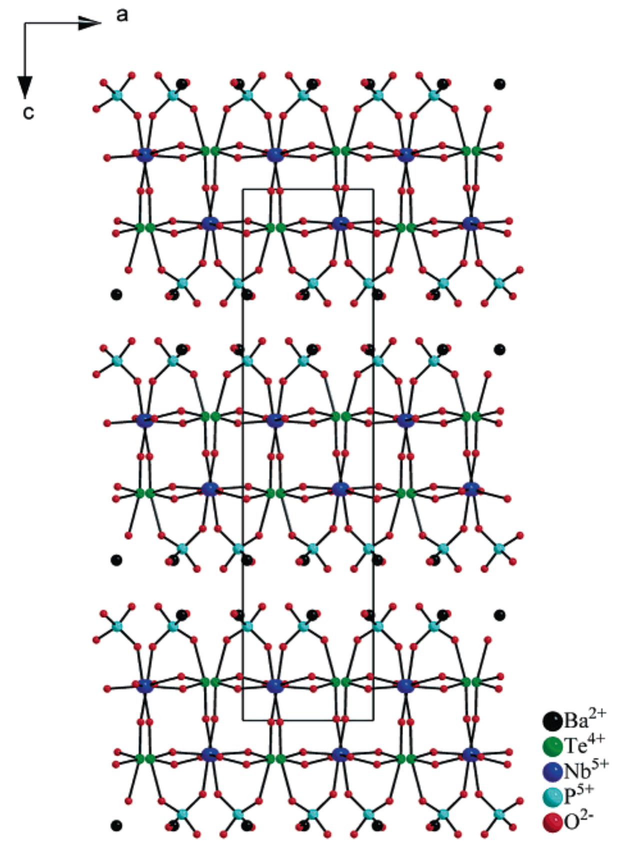

Figure 2. Ball-and-stick diagram of $BaTeNbO_4(PO_4)$ in the *ac* plane. Note the layered structure consisting of NbO_6 octahedra, TeO_4 polyhedra, and PO_4 tetrahedra.

One of the interesting aspects in the reported materials is the intraoctahedral distortion of the Nb^{5+} cation. This out-

---

(31) Brown, I. D.; Altermatt, D. *Acta Crystallogr.* **1985**, *B41*, 244.
(32) Brese, N. E.; O’Keeffe, M. *Acta Crystallogr.* **1991**, *B47*, 192.

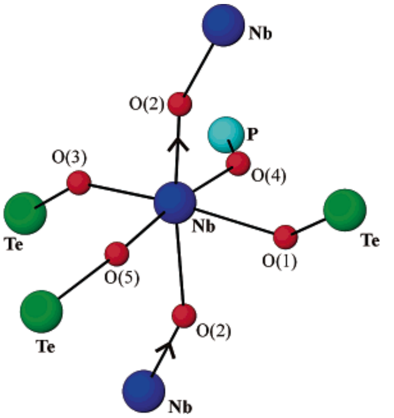

Figure 3. Ball-and-stick representation of the local coordination environment of a NbO$_6$ octahedron in BaTeNbO$_4$(PO$_4$). The arrow represents the direction of the intra-octahedral distortion for the Nb^{5+} cation.

of-center distortion is attributable to second-order Jahn−Teller (SOJT) effects[21−25,33] (electronic effects) and can be considered as a primary distortion for the cation. Secondary distortions also occur and are attributable to bond networks and lattice stresses in the solid-state framework.[34,35] For BaTeNbO$_4$(PO$_4$), these secondary distortions are between the NbO$_6$ octahedron and the PO$_4$ and TeO$_4$ polyhedra. Two aspects of the intraoctahedral distortion, the direction and magnitude, can be understood using primary and secondary distortion concepts. As previously shown, the intraoctaheral distortion can occur along the local C_2, C_3, or C_4 direction of the octahedron, i.e., toward the edge, face, or corner.[36] For Nb^{5+}, all three distortional directions can occur, but a C_4-Nb^{5+} is the most common. In addition, the magnitude of the C_4-Nb^{5+} distortion is weaker than the analogous C_4-V^{5+}, C_4-Mo^{6+}, and C_4-W^{6+} distortion, but is stronger than C_4-Ta^{5+} and C_4-Ti^{4+} distortions.[37] The primary distortion, attributable to SOJT or electronic effects, influences the magnitude of the cationic displacement, since this magnitude is related to the HOMO−LUMO gap as well as the electronegativity of the cation. The secondary distortion reinforces the direction of the out-of-center displacement. This secondary effect is, however, more subtle. If we examine the NbO$_6$ octahedron in BaTeNbO$_4$(PO$_4$), we note that the Nb^{5+} cation distorts in the local C_4 direction toward O(2) (see Figure 3). This distortion is represented by an arrow in Figure 3. The remaining oxygen atoms, O(1), O(3), O(4), and O(5), bridge Nb^{5+} to either a P^{5+} or a Te^{4+} cation. The question arises: Why does Nb^{5+} distort toward O(2) and not toward any of the other oxide ligands? Bond valence calculations[31,32] on the oxide ligands around Nb^{5+} result in values ranging from 1.815 to 2.199. Interestingly, O(2) has a bond valence of 1.934, whereas O(4) has the lowest bond valence of 1.815. If Nb^{5+} were to distort toward any of the other oxide ligands, e.g., O(4) or O(3) and O(5), an additional distortion within the PO$_4$ or TeO$_4$ polyhedra would be necessary. In other words, decreasing one or more of the Nb−O bonds would simultaneously increase the adjacent P−O or Te−O bond. At present, P^{5+} is in a regular tetrahedral environment, with P−O bond lengths ranging from 1.519(5) to 1.561(5) Å and O−P−O bond angles between 106.8(3)° and 110.3(3)°. Any substantial change in a P−O bond would distort, and likely destabilize, the PO$_4$ tetrahedra. Thus, there does not seem to be any driving force for such a tetrahedral distortion. A similar situation occurs with the TeO$_4$ polyhedra. The TeO$_4$ group is already in a “predistorted” asymmetric coordination environment attributable to the lone pair on Te^{4+}. A further distortion of the Te^{4+} cation would either increase the lone pair−oxide or oxide−oxide interactions, both of which would be structurally unfavorable. Since a displacement of Nb^{5+} toward O(1), O(3), O(5), or O(6) would produce unfavorable distortions in the PO$_4$ or TeO$_4$ polyhedra, the only remaining option for Nb^{5+} is to distort away from these oxygen atoms and toward O(2), i.e., a C_4-Nb^{5+} distortion. Thus, the secondary distortion, attributable to the interactions between the PO$_4$ and TeO$_4$ polyhedra with the NbO$_6$ octahedron, reinforces the direction of the Nb^{5+} displacement.

Table 4. Infrared and Raman Vibrations for BaMTeO$_4$(PO$_4$) (M = Nb or Ta)

IR (cm^{-1})				Raman (cm^{-1})			
P−O	M−O	Te−O	M−O−Te	P−O	M−O	Te−O	M−O−Te
			BaNbTeO$_4$(PO$_4$)				
1101	981	800	644	1088	949	779	671
1066	904	690		905	831	610	
944	565				567		
	536						
			BaTaTeO$_4$(PO$_4$)				
1103	983	802	649	1098	957	782	679
1070	916	673		918	849	617	
956	563				565		
	539						

Infrared and Raman Spectroscopy. The infrared and Raman spectra of BaTeMO$_4$(PO$_4$) (M = Nb or Ta) revealed P−O, M−O, Te−O, and M−O−Te vibrations. P−O vibrations are observed in both the IR and Raman and occur between 940 and 1100 cm^{-1}. M−O and Te−O vibrations are also observed in both the IR and Raman and found around 900−980 and 670−800 cm^{-1}, respectively. Multiple bands, occurring around 640−670 cm^{-1}, are attributable to M−O−Te vibrations. The infrared and Raman vibrations and assignments for BaTeMO$_4$(PO$_4$) are listed in Table 4. The assignments are consistent with those previously reported.[38−41]

Thermogravimetric Analysis. The thermal behavior of BaTeMO$_4$(PO$_4$) (M = Nb or Ta) was investigated using thermogravimetric analysis. BaTeMO$_4$(PO$_4$) were not stable at higher temperature. In each case, a single step decomposition occurs indicating volatilization above 770 °C for

---

(33) Pearson, R. G. *J. Am. Chem. Soc.* **1969**, *91*, 4947.
(34) Kunz, M.; Brown, I. D. *J. Solid State Chem.* **1995**, *115*, 395.
(35) Welk, M. E.; Norquist, A. J.; Arnold, F. P.; Stern, C. L.; Poeppelmeier, K. R. *Inorg. Chem.* **2002**, *41*, 5119.
(36) Goodenough, J. B. *Annu. Rev. Mater. Sci.* **1998**, *28*, 1.
(37) Halasyamani, P. S. In preparation.
(38) Baltes, M.; Kytokivi, A.; Weckhuysen, B. M.; Schoonheydt, R. A.; Van Der Voort, P.; Vansant, E. F. *J. Phys. Chem. B* **2001**, *105*, 6211.
(39) Javier Cabello Sanchez, F.; Wells, R. P. K.; Rhodes, C.; Bartley, J. K.; Kiely, C. J.; Hutchings, G. J. *Phys. Chem. Chem. Phys.* **2001**, *3*, 4122.
(40) Durga, D. K.; Veeraiah, N. *J. Phys. Chem. Solids* **2003**, *64*, 133.
(41) Sudarsan, V.; Muthe, K. P.; Vyas, J. C.; Kulshreshtha, S. K. *J. Alloys Compd.* **2002**, *336*, 119.

$BaTeNbO_4(PO_4)$ and 800 °C for $BaTeTaO_4(PO_4)$. Powder XRD measurements on the calcined materials revealed $BaTeMO_4(PO_4)$ decomposed to a mixture of $Nb_2Te_3O_{11}$[42] (or $Ta_2Te_3O_{11}$)[43] and unknown amorphous materials.

Ion-Exchange Experiments. At present, we have been unable to successfully ion-exchange the Ba^{2+} cations. The reactions attempted at 80 °C for 3 days in aqueous nitrate solution did not exchange the metal. However, the reactions performed in sealed fused silica tube with wet chloride salts at 120 °C for 4 days produced crystals of $CaNb_2O_6$[44] and $Ca_2(PO_4)Cl$[45] by decomposition reactions. We are continuing to investigate the ion-exchange properties of the reported materials.

Acknowledgment. We thank the Robert A. Welch Foundation for support. This work was also supported by the NSF-Career Program through DMR-0092054, and an acknowledgment is made to the donors of the Petroleum Research Fund, administered by the American Chemical Society, for partial support of this research. P.S.H. is a Beckman Young Investigator. We also acknowledge Jason Locklin and Prof. Rigoberto Advincula for assistance in obtaining the Raman spectra. J.O. acknowledges the 2003 NSF Summer Research Program in Solid State Chemistry (DMR-0303450) for support.

Supporting Information Available: X-ray crystallographic files for $BaTeNbO_4(PO_4)$ in CIF format and calculated and observed X-ray diffraction patterns for $BaTeNaO_4(PO_4)$ and $BaTeTaO_4(PO_4)$. This material is available free of charge via the Internet at http://pubs.acs.org.

IC0350335

---

(42) Bart, J. C. J.; Petrini, G. *Z. Anorg. Allg. Chem.* **1980**, *466*, 81.
(43) Bart, J. C. J.; Petrini, G. *Z. Anorg. Allg. Chem.* **1980**, *465*, 51.
(44) Cummings, J. P.; Simonsen, S. H. *Am. Mineral.* **1970**, *55*, 90.
(45) Greenblatt, M.; Banks, E.; Post, B. *Acta Crystallogr.* **1967**, *23*, 166.